PHYSICAL REVIEW B **77**, 180401(R) (2008)

Excitation of coupled oscillations in lateral ferromagnetic heterostructures

Nikolay I. Polushkin
Institute for Physics of Microstructures, Russian Academy of Sciences, 603950 GSP-105 Nizhniy Novgorod, Russia
(Received 7 April 2008; revised manuscript received 18 April 2008; published 12 May 2008)

The intensities of spin-wave (magnetostatic) modes in thin ferromagnetic films and laterally confined structures are usually insensitive to their dimensions. We observe a strong dependence of the resonant microwave absorption in periodic heterostructures of closely packed ferromagnetic stripes on the structure period p. The obtained experimental data supported by computing the mode profiles indicate the existence of unusual standing waves, which are collective magnetostatic modes excited in the heterostructures by a uniform rf magnetic field. These stationary states result from superposition of the spin waves propagating in opposite directions and having wave numbers of $\pm 2\pi l/p$, where l are integers.

DOI: 10.1103/PhysRevB.77.180401 PACS number(s): 76.50.+g, 75.30.Ds, 75.40.Gb

Coherent excitation of coupled oscillators is an intriguing phenomenon occurring in both physical and biological systems.[1] A striking feature inherent to a simplest system with two linear oscillators (coupled pendulums) is that they are able to synchronously resonate either in phase (acoustic mode) or antiphase (optic mode).[2] These modes persist in systems of many coupled oscillators such as (ferro)magnetic multilayer structures[3] where the magnetic coupling between the layers (oscillators) gives rise to the high-frequency precession modes,[4] which thus provide new functionalities for structured ferromagnetic materials.[4,5] Nearly four decades ago, Hoffman *et al.*[6] proposed a concept of exchange coupling at the interface between the two ferromagnetic layers. This concept has been modified by Grünberg[7] who considered the effects of interlayer magnetostatic coupling, which is caused by stray fields generated by the spin motions, on the spin-wave properties of a bilayer film with a nonmagnetic spacer. More recently, magnetostatic coupling was found in laterally confined structures, notably periodic arrays of closely packed submicron stripes[8] and dots.[9] A common manifestation of the coupling is the occurrence of *collective* spin excitations in the structures where the spacing between adjacent elements is sufficiently small.[10]

While all the previous work dealt with *discrete* lateral structures, we explore *continuous* structures that consist of periodically arranged blocks (stripes) with different magnetic properties, notably the saturation magnetization (magnetization) $4\pi M$.[11,12] In the absence of separation between adjacent stripes in our structures, spin oscillations can *easily* transfer from one its constituent with a magnetization of $4\pi M_1$ to another one with a magnetization of $4\pi M_2$. In our earlier studies of such structures with submicron periodicities (~ 0.9 μm), we found experimental evidences of the collective spin precession optically excited with a wave number $k_0 \ll \pi/p$ (p is the structure period).[12] Here, we use a uniform rf magnetic field ($k_0 \to 0$) in the standard geometry of ferromagnetic resonance (FMR) to demonstrate that the coupled oscillations are excited in our structures with much larger periodicities, with even up to tens of micrometers. Due to its excellent sensitivity, the FMR method unambiguously provides the information about the structures in a wide range of their periodicities. The aim of this Rapid Communication is to study the coupling effects at different structure parameters such as the structure period, stripe thickness, and width. These studies reveal the existence of unusual standing waves that are magnetostatic modes extended through a whole heterostructure period. In their lowest order (acousticlike oscillations), such collective standing-wave modes have nonzero minima of the oscillation amplitude instead of the nodes. The distances between neighboring nodes in the higher-order modes (opticlike and hybrid oscillations) are shorter than those in usual standing waves. Experimentally, we observe a strong dependence of the resonant microwave absorption (MA) on the structure period, which contrasts to typical resonance behavior of thin ferromagnetic films.[13] Computation of the FMR linear response allows us to assign the observed MA resonances to the specific oscillation types and finally indicates the occurrence of the collective standing-wave modes.

The samples studied are lateral structures with one-dimensional periodic modulation of $4\pi M$ in a layer whose thickness t is much smaller than the modulation period p. The structures were produced by direct laser interference patterning of thin-film (0.01–0.1 μm) Fe_XV_{1-X} ($X=0.6-0.8$) mixtures prepared on Si substrates. It is argued in Refs. 11 and 12 that nanosecond laser annealing causes an increase in the magnetization of phase-separating Fe-based alloys and that annealing by two interfering laser beams causes this increase mostly in one-dimensional maxima of the light intensity. Figure 1(a) shows a typical magnetic force microscopy (MFM) image of a patterned $Fe_{0.7}V_{0.3}$ sample. The initial saturation magnetization of this sample was $4\pi M = 6.3$ kG. The vertical dark and bright lines distinctively seen in the top inset of Fig. 1(a) are the north and south magnetic poles (labeled N and S), which indicate the interfaces between the stripes having different magnetizations, $4\pi M_1$ and $4\pi M_2$, as schematically illustrated in the bottom inset of Fig. 1(a). To saturate magnetizations in the stripes of both kinds and thus to render the poles more pronounced, a magnetic field of 300 Oe was applied *in situ* along the direction of periodicity. It is important that MFM data allow to evaluate not only the structure period but also the widths of the stripes, w_1 and w_2, with plotting $r=w_1/p$ as a function of laser intensity Φ [Fig. 1(b)]. Then, it is possible to determine w_1 and w_2. For instance, $r=0.35\pm0.05$ for the sample in Fig. 1(a).

The FMR data were taken at $\omega/2\pi = 9.5$ GHz by monitoring the derivative of the MA as a function of a static field $\vec{H}_0$

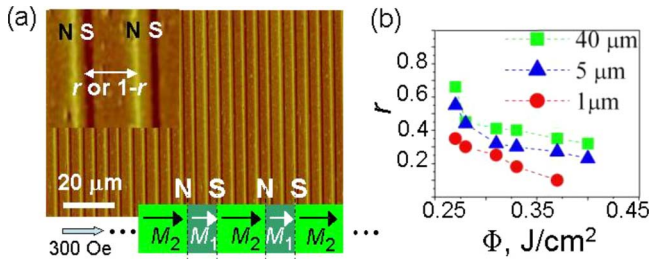

FIG. 1. (Color online) (a) MFM image of a patterned Fe-V sample. N and S denote the magnetic poles. The values r (or $1-r$) and p can be determined from N-N and N-S distances. The inset in bottom of (a) illustrates schematic distribution of the magnetization in the stripe structures. (b) The ratio of stripe width to structure period $r=w_1/p$ as a function of laser intensity Φ for different interference periods, $p=40$, 5, and 1 μm.

applied to a sample mounted inside a TE_{102} microwave cavity. All the patterned samples subjected to these studies had the same sizes, 1.0×1.0 mm^2. Figures 2(a)–2(d) show MA spectra of the stripe structures patterned with three different periodicities, (a) $p=100$, (b) 20, and [(c) and (d)] 10 μm, and with two different ratios of stripe width to period, $r=0.35$ [(a)–(c)] and 0.20 (d) in a $Fe_{0.7}V_{0.3}$ layer of a thickness of $t=0.1$ μm. These spectra were obtained by integrating the derivative of Im χ on H_0, and the MA was measured at different angles ϕ of orientation of the direction of periodicity with respect to $\vec{H}_0$ (inset of Fig. 2). All of the plots in Fig. 2 clearly show the two strong absorption lines of a width of ~100 Oe, which are labeled as "1" and "2," that dominate in the spectra. In a rough approximation, it is reasonable to attribute the resonances 1 and 2 to the individual precession of the magnetizations $4\pi M_1$ and $4\pi M_2$. For larger p (~100 μm), the positions of these resonances are in good agreement with the well-known Kittel formula given in the textbooks. In addition to the two basic resonances, a series of additional absorption peaks develops in the spectra to be most pronounced at $p<20$ μm and ϕ close to 90°. The

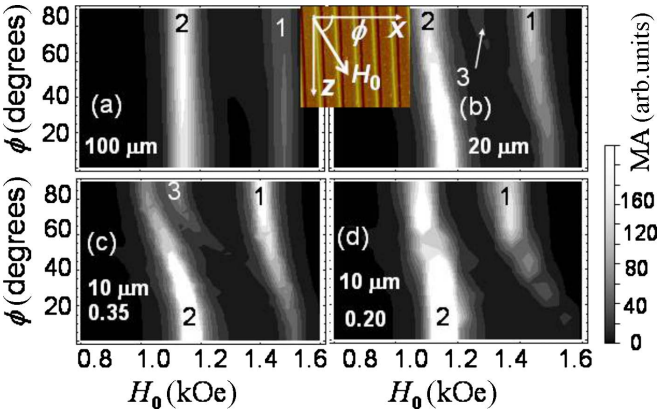

FIG. 2. (Color online) Microwave absorption as a function of ϕ in a 0.1 μm thick sample patterned with different periodicities: (a) $p=100$, (b) 20 μm, and [(c) and (d)] 10 μm and with different ratios of stripe width to period (a)–(c) $r=0.35$ and (d) 0.20. Up to three strongest resonances labeled "1," "2," and "3" are marked. The inset illustrates the geometry of the experiments.

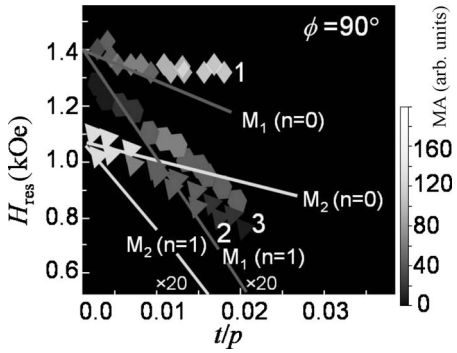

FIG. 3. Three-dimensional plot of normalized peak intensities and positions measured at $\phi=90°$ and shown by symbols for the three strongest resonances versus t/p ($t=0.1$ μm) at constant $r=0.35$. For the lines labeled M_1 and M_2, see the text. The peak intensities are shown by scaled gray tones.

strongest of this series labeled as "3" appears between the positions of the basic lines 1 and 2 [Figs. 2(b) and 2(c)]. Other additional peaks are much weaker than these three and not shown here. The observed multiple features can be associated with the standing-wave dipolar resonances that result from quantizing the wave vector directed along the width of a stripe.[14]

Here, it is essential that the intensities and positions of the observed resonances strongly depend on the ratio of t/p. Figure 3 shows the normalized peak intensities and positions H_{res} measured at $\phi=90°$ for the three strongest resonances 1, 2, and 3 as functions of t/p at $t=0.1$ μm and $r=0.35$. These data are shown by symbols, with indication of the peak intensities shown by scaled gray tones. We see that the intensity of resonance 2 is much smaller than that of resonance 1 at $t/p>0.01$, while the ratio between their intensities is opposite at $t/p<0.005$. It is also striking that the basic resonance 2 is vanishing at $t/p>0.02$, while the additional resonance labeled 3 still persists at large t/p. The measured peak intensities and positions are compared to those in the calculated MA spectra for individual stripes having the same dimensions. To calculate these spectra, we used a linear-response theory developed here and applied to periodic arrays of ferromagnetic stripes separated from each other by nonmagnetic (NM) spacers. For the calculation, the parameters of these structures were chosen as follows: $4\pi M_1=6.3$ kG and $4\pi M_2=8.8$ kG, the stripe widths are, respectively, $w_1=rp$ and $w_2=(1-r)p$ in the structures labeled as M_1/NM, NM/M_2 through the text and M_1, M_2 in Fig. 3, where $r=0.35$, the damping constant $\alpha=0.01$, and the gyromagnetic ratio $\gamma/2\pi=2.8$ GHz/kOe. The factor of t/p was varied in the range of 10^{-3}–10^{-1}. The solid lines indicate the peak intensities and positions of the two lowest modes, $n=0$ and $n=1$, for the structures M_1/NM (M_1) and NM/M_2 (M_2). The peak intensities of the mode $n=1$ are amplified by a factor of 20. In contrast to the measured dependences shown by symbols, all the solid lines have a uniform gray tone. This indicates a basic difference between the resonance behavior of the structures M_1/M_2 and that of the structures with separated stripes where the resonance intensities are insensitive to the stripe dimensions. Another fact is that the

positions of the resonances 1 and 2, H_{res}, are shifted, respectively, to higher and lower resonance fields with respect to the main resonances ($n=0$) for the structures M_1/NM and NM/M_2, especially for large t/p.

Finally, note that the FMR spectra were also measured for the films with different stripe thicknesses from $t=0.1$ μm to $t=0.01$ μm. It is striking that no changes in the peak intensities normalized to those calculated for individual stripes occur when t and p are varied in *proportion* to each other (i.e., t/p is constant) at constant r.[15] Such behavior indicates that the dimensionless factor of t/p plays a role in the magnetization dynamics of the structures under study.

To explain the observed behaviors, computation of the FMR response has been performed upon the basis of linearized equation for the amplitude of dynamic magnetization $\vec{m}$ given in the Landau-Lifshitz-Gilbert (LLG) form with neglecting exchange,[16] notably $i\Omega 4\pi m_{\parallel}(x)=-M(x)h_y(x)+\Omega_H 4\pi m_y(x)$ and $i\Omega 4\pi m_y(x)=M(x)h_x(x)\sin\phi-\Omega_H 4\pi m_{\parallel}(x)+M(x)h_{e\parallel}$. In these equations, $m_{\parallel}$ and m_y are the in-plane and vertical components of $\vec{m}$, h_x and h_y are the components of the dynamic stray field related to $\vec{m}$ in accordance with Maxwell's equation $\nabla\vec{h}=-4\pi\nabla\vec{m}$, $h_{e\parallel}$ is the in-plane amplitude of the rf field having a frequency ω, $\Omega=\omega/(4\pi\gamma)$, $\Omega_H=(\gamma H+\alpha i\omega)/(4\pi\gamma)$, and $H=H_0+H_{dx}$, where H_{dx} is the static demagnetizing field. The coordinate system x, y, and z used is shown in the inset of Fig. 2. Since $t\ll p$ under the experimental conditions used, one can neglect both the H_{dx} with its effects (even at $\phi=0°$, where H_{dx} reaches its maximum) and the dependence of the dynamic fields on y. We assume that the stripe length is much larger than their width [Fig. 1(a)], so the static magnetization $\vec{M}$ and dynamic fields $\vec{m}$ and $\vec{h}$ are functions of a single spatial variable x. Also, one assumes that $\vec{M}(x)$ has a rectangular distribution over the period and is oriented along $\vec{H}$. Since $M(x)$ is periodic and pumping of its precession is uniform, the dynamic magnetization can be sought as a plane-wave expansion,

$$\vec{m}(x)=\sum_{l=-\infty}^{\infty}\vec{m}_l\exp(iqlx), \tag{1}$$

where the wave numbers are $\pm|l|q$, l are integers, and $q=2\pi/p$. Then, the components of $\vec{h}$ can be expressed as[14]

$$h_{x(y)}=-4\pi\sum_{l=-\infty}^{\infty}m_{x(y)l}P_{x(y)l}\exp(iqlx), \tag{2}$$

where $P_{yl}=[1-\exp(-|l|qt)]/|l|qt$ and $P_{x(l)}=1-P_{y(l)}$ are the dynamic demagnetizing factors. Substituting all of the expansions [including a Fourier expansion of $M(x)$] into the LLG equations, we obtain an infinite set of linear algebraic equations with respect to the Fourier components of the in-plane dynamic susceptibility $\chi_k=4\pi m_k/h_e$ (the index $\parallel$ here is omitted)

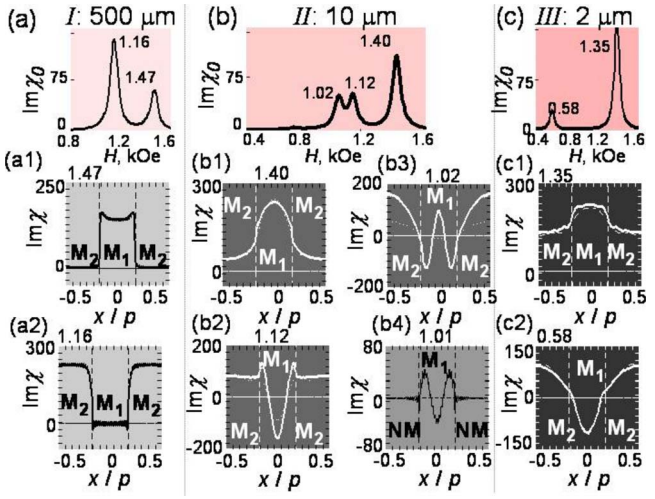

FIG. 4. (Color online) (a)–(c) MA spectra calculated at $\phi=90°$ for the structures M_1/M_2 with periodicities of $p=500$ (structure I) and 10 μm (structure II), and 2 μm (structure III). (a1)–(c2) Resonant mode profiles for the structures I (a1, a2), II (b1, b2, b3), III (c1, c2), and for the structure M_1/NM with $p=10$ μm (b4).

$$\sum_{k=-\infty}^{\infty}(A_{kl}-\lambda\delta_{k,l})\chi_k=B_l, \tag{3}$$

where $A_{kl}=(C_{kl}-P_kD_{kl})\sin^2\phi+\Omega_H P_k M_{l-k}\cos^2\phi$, $C_{kl}=\Omega_H M_{l-k}+\Sigma_{s=-\infty}^{\infty}M_l M_{s-k}P_s$, $D_{kl}=C_{kl}-\Omega_H M_{l-k}$, $\lambda=\Omega^2-\Omega_H^2$, and $B_l=C_{k,l}\delta_{k,0}$. This set has been numerically solved by retaining a finite number (up to ~50) of the Fourier components of $M(x)$ and finding $\chi_k(H)=\Delta_k(H)/\Delta(H)$, where Δ is the determinant of the matrix A_{kl} and Δ_k is the determinant obtained by replacing the kth column by B_l.

The obtained solution provides the information about not only the MA $\propto \mathrm{Im}\,\chi_0$ as a function of H [Figs. 4(a) and 4(c)] but also about the resonant distribution of Im χ over the period (the mode profile) [Figs. 4(a1)–4(c2)] obtained by summation of the Fourier series at $H=H_{res}$. Theoretically, we study the structures with three different periods, $p=500$ (structure I), 10 (structure II), and M_1/NM and 2 μm (structure III), but with the same $r=0.35$. One of them (II) was experimentally studied, and its spectrum was shown in Fig. 2(c). The other parameters taken for this computation correspond to those used in the experiments.

In the system M_1/M_2 with noninteracting stripes, the stripes with the magnetization $4\pi M_1$ (subsystem M_1) could not be excited at the applied field H being tuned to excite the stripes with the magnetization $4\pi M_2$ (subsystem M_2) and vice versa. Indeed, no off-resonance absorption, which would exceed a computation error (~10%), is marked in the structure I having a comparatively large period [Figs. 4(a1) and 4(a2)]. However, all of the mode profiles for the structures with smaller periods, II [Figs. 4(b1), 4(b2), 4(b3)] and furthermore III [Figs. 4(c1) and 4(c2)], clearly indicate the interstripe coupling. In other words, *both the subsystems start to oscillate when H is tuned to any of the resonances* at 1.40, 1.12, 1.02 [Fig. 4(b)], or 1.35, and 0.58 kOe [Fig. 4(c)] for structures II and III, respectively. We mark three different

regimes of the interstripe coupling. In the first of them, the resonant absorption Im $\chi > 0$ everywhere inside both the media, so the subsystems M_1 and M_2 oscillate in phase with respect to each other [Figs. 4(b1) and 4(c1)]. This oscillation regime can be referred to as the *acoustic* mode. In the second regime, the majority of magnetic moments in the M_1 oscillate in antiphase to those in the M_2. Such oscillations can be referred to as the *optic* mode that contains the two nodes (Im $\chi=0$) within the period, which are located at $\pm 0.09p$ and $\pm 0.14p$ in structures II [Fig. 4(b2)] and III [Fig. 4(c2)], respectively. In the third regime, the mode is *hybridized* as containing up to the four regions in which alternately Im $\chi > 0$ and Im $\chi < 0$ [Fig. 4(b3)], with the four nodes located at $\pm 0.05p$ and $\pm 0.20p$ in structure II. The profile of the hybrid mode in Fig. 4(b3) should be compared to that of the mode $n=1$ in the structure M_1/NM [Fig. 4(b4)]. As seen, the oscillations inside the M_1 in the hybrid mode are excited in antiphase with respect to those in the mode $n=1$. In addition, their intensity is higher by a factor of 3 than that of the mode $n=1$ in the structure M_1/NM. These differences prove the collective nature of the oscillations in the hybrid mode. Interestingly, other absorption peaks in structure II, which are weaker and located at lower resonance fields (not shown), can be assigned to higher-order hybrid modes, as these exhibit more oscillations in the sign of Im χ inside both the M_1 and M_2. In terms of standing-wave resonances, a higher index may be assigned to a hybrid mode than that to acoustic and optic modes.

As follows from Eq. (1), the mode profiles shown in Fig. 4 result from superposition of the waves propagating in the two opposite directions along the x axis. These stationary states are unusual standing waves as having nonzero minima of the oscillation amplitude instead of the nodes in the acoustic mode or the distances between neighboring nodes in the higher (optic and hybrid) modes are shorter than those in usual standing waves at the same periodicity.

Computation of the mode profiles shown in Fig. 4 allows us to understand the anomalous behavior of the resonance intensities in the structures M_1/M_2. Since the MA $\propto$ Im χ_0, while Im χ_0 is equal to Im $\chi(x)$ averaged over the structure period, the antiphase oscillations of the M_1 and M_2 in the optic mode, where, respectively, Im $\chi < 0$ and Im $\chi > 0$, cancel each other, thus providing reduction of the MA [Figs. 4(b2) and 4(c2)]. As hybrid modes contain multiple regions in which both Im $\chi < 0$ and Im $\chi > 0$, the index of any of them should be higher than that of the optic mode, so even the lowest hybrid resonance, 2, may be weaker in its intensity than the optic resonance, 3. This is consistent with our observations. In contrast to the optic and hybrid resonances, the in-phase oscillations of the two subsystems (everywhere Im $\chi > 0$) result in the enhanced intensity of the acoustic resonance [Fig. 4(b1) and 4(c1)].

With ϕ varied from 90° to 0°, only a magnetostatic-field component h_y is nonvanishing. As h_y is generated by m_y, which is much smaller than the in-plane component of $\vec{m}$, the coupling effect becomes less pronounced in the geometries different from $\phi=90°$. In the geometry $\phi=0°$, for instance, we mark a relatively much weaker dependence of the resonance intensities on p (Fig. 2).

In summary, we propose how to modify the design of lateral ferromagnetic structures for effective excitation of the coupled magnetic oscillations in them. The coupling mediates the strong changes in the intensities of resonance modes with a varied factor of t/p. The developed formalism for calculation of the linear FMR response casts light on the nature of the observed resonances and indicates the existence of unusual standing waves that are collective magnetostatic modes. These findings enhance understanding of the magnetism of mesoscopic systems and point to a kind of artificially structured materials with possible applications to microwave technology.

This work was supported by the Russian Foundation of Basic Research (Grant No. 07-02-01305).

[1] M. Rosenblum and A. Pikovski, Contemp. Phys. **44**, 401 (2003), and references therein.
[2] M. I. Rabinovich and D. I. Trubetskov, *Oscillations and Waves in Linear and Nonlinear Systems* (Springer, Berlin, 1989).
[3] R. E. Camley and R. L. Stamps, J. Phys.: Condens. Matter **5**, 3727 (1992).
[4] R. J. Astalos and R. E. Camley, Phys. Rev. B **58**, 8646 (1998).
[5] B. Kuanr, I. R. Harward, D. L. Marvin, T. Fal, R. E. Camley, D. L. Mills, and Z. Celinski, IEEE Trans. Magn. **41**, 3538 (2005).
[6] F. Hoffman, A. Stankoff, and H. Pascard, J. Appl. Phys. **41**, 1022 (1970).
[7] P. Grünberg, J. Appl. Phys. **51**, 4338 (1980).
[8] G. Gubiotti, S. Tacchi, G. Carlotti, P. Vavassori, N. Singh, S. Goolaup, A. O. Adeyeye, A. Stashkevich, and M. Kostylev, Phys. Rev. B **72**, 224413 (2005); G. Gubiotti, S. Tacchi, G. Carlotti, N. Singh, S. Goolaup, A. O. Adeyeye, and M. Kostylev, Appl. Phys. Lett. **90**, 092503 (2007).
[9] S. Jung, B. Watkins, L. DeLong, J. B. Ketterson, and V. Chandrasekhar, Phys. Rev. B **66**, 132401 (2002).
[10] M. P. Kostylev, A. A. Stashkevich, and N. A. Sergeeva, Phys. Rev. B **69**, 064408 (2004); R. Arias and D. L. Mills, *ibid.* **67**, 094423 (2003).
[11] N. I. Polushkin, S. A. Gusev, M. N. Drozdov, Y. K. Verevkin, and V. N. Petryakov, J. Appl. Phys. **81**, 5478 (1997).
[12] N. I. Polushkin, S. A. Michalski, L. Yue, and R. D. Kirby, Phys. Rev. Lett. **97**, 256401 (2006).
[13] M. Sparks, Phys. Rev. B **1**, 3831 (1970).
[14] K. Y. Guslienko, S. O. Demokritov, B. Hillebrands, and A. N. Slavin, Phys. Rev. B **66**, 132402 (2002).
[15] Of course, the resonance intensities alter with changing r at constant t/p, as shown experimentally in Figs. 2(c) and 2(d).
[16] As its contribution to the precessional dynamics on the spatial scale of the structures under studies is much smaller than that of the external and demagnetizing fields, nonuniform exchange can be neglected in the LLG equation.